Introduction

Optimal field development and management process operates on critical decision variables, such as well locations and control settings, to maximize an economic objective function. However, mathematically this results in a high-dimensional, constrained optimization problem with computationally demanding and uncertain objective function (i.e. the production forecast model and field performance estimates based on it). The control variables in this optimization problem can be grouped based on their type (e.g. integer well locations, continuous well production or injection control settings). Each such group is referred to as an *optimization level* in this paper.

Single-level optimization frameworks have been developed, and optimize only one type of decision variables (a.k.a. 'control variables'), such as well locations (Al-Ismael et al. 2018, Wang et al. 2012, Li and Jafarpour 2012), drilling order (Tavallali et al. 2018), or well production/injection control settings (a.k.a. 'well control settings') like flow rate or pressure (Jiang et al. 2019, Haghighat Sefat 2016). These methods may not be appropriate where the optimization problem involves multiple levels, because these methods do not capture the potential correlations or interference among control variables at different levels. In contrast, multi-level frameworks aim to simultaneously optimize multiple types of variables at different levels to account for the correlation among control variables. Current multi-level approaches can be classified into two groups: (1) *Joint optimization* (Isebor et al. 2014, Shirangi et al. 2018, Lu and Reynolds 2019): a single augmented vector containing all control variables at different levels is optimized. A sub-optimal solution is expected when using this approach in reasonable-scale full-field applications due to the optimization algorithm's high demand for computational resources because of the large number of simultaneous control variables. (2) *sequential optimization* (Li et al. 2013, Forouzanfar et al. 2016, Lu et al. 2017a): in this approach the main problem is divided into sub-problems with reduced number of control variables. Each sub-problem is a single-level optimization (with a single type of control variable); an iterative approach is then employed to account for the correlations among control variables at different levels.

Current field development/control optimization frameworks can further be classified into three main groups based on the employed optimization algorithm: (1) stochastic derivative-free and metaheuristic [e.g. using genetic algorithm (Güyagüler et al. 2002, Almeida et al. 2010) or particle swarm optimization algorithm (Harb et al. 2019)], (2) adjoint gradient-based (Sarma et al. 2005, Van Essen et al. 2011), and (3) stochastic approximated gradient-based [e.g. using Simultaneous Perturbation Stochastic Approximation (SPSA) (Li et al. 2013) or Stochastic Simplex Approximate Gradient (StoSAG) method (Fonseca et al. 2017)]. Stochastic derivative-free and metaheuristic algorithms can globally search for the optimal solution of all types of control variables (e.g. categorical, integer, continuous), however they typically have a slower convergence rate than gradient-based algorithms and their performance decreases rapidly with increasing number of control variables (Zingg et al. 2008). Adjoint gradient-based methods are computationally efficient, however access to the reservoir simulation source code is required for efficient calculation of the gradient which makes them impractical for use with commercial reservoir simulators. Approximate gradient-based algorithms are developed to address this issue by stochastically estimating the gradient of a black-box objective function using an ensemble of simultaneous perturbation of all control variables. The approximate gradient-based algorithms have been successfully employed to solve large-scale well placement [e.g. (Jesmani et al. 2016) using SPSA] and well control problems [e.g. (Sefat et al. 2016) using SPSA and (Lu et al. 2017b) using StoSAG].

The reservoir model is never perfect, nor the production forecast based on it. Hundreds of reservoir model realizations are generally developed to quantify the underlying uncertainty due to limited reservoir description knowledge. A robust, optimal well placement/control solution can then be achieved by optimising the expected value of the objective function over the ensemble of model realizations. A variety of techniques have been developed to select a relatively small ensemble of model realizations, as the sufficient representative of all possible realizations for the problem at hand, to reduce the computation time associated with the robust optimization process. Note that the random sampling techniques (e.g. Chen et al. (2012)) cannot guarantee capturing the underlying uncertainty. Iteratively updating the randomly selected samples during the optimisation process (e.g. Lu et al. (2017a)) can

potentially improve the performance especially with a large number of iterations. A systematic selection technique (Wang et al. 2012, Sefat et al. 2016) is preferred to select a subset of realizations as the representative of all realizations, tailored to the objective of the subsequent optimization.

Current single/multi-level optimization frameworks provide a single solution as the output, while in practice, operational problems often impose unexpected constraints that result in operators having to adjust the optimal solution degrading its value. For instance, the provided optimal well location solution could be impractical (or difficult) to drill, due to the deviation of the well trajectory from the planned trajectory, caused by operational/tool errors. Hence operational flexibility is an outstanding challenge to be addressed for practical application of the optimization frameworks.

This paper presents a multi-solution optimization framework (MSOF) to solve well placement and control problems under geological uncertainty, based on a multi-level sequential (iterative) approach. SPSA is used as the optimizer, while gradients at each iteration are estimated using a 1:1 ratio between the ensemble of control variables perturbations and the ensemble of selected model realizations. An ensemble of close-to-optimum solutions is then chosen from each level (e.g. from the well placement optimization level), transferred to the next level of optimization (e.g. where the well controls are optimized), and this loop continues until no significant improvement is observed in the expected objective value. Fit-for-purpose clustering procedures are developed to systematically select an ensemble of realizations to capture the underlying model uncertainties, as well as an ensemble of solutions with adequate differences in control variables but close-to-optimum objective values, at each optimization level.

This paper is organized as follows: First, problem formulation for robust well placement/control optimization, with an uncertain reservoir model, is presented; followed by a brief description of the SPSA algorithm. Next, the developed techniques for reservoir model realization selection as well as multi-solution selection at each optimization level are presented. The MSOF is then presented and applied to a benchmark case study (Brugge oil field model) followed by discussion of the results and conclusions.

Problem statement

In this work, the objective is to find optimal set(s) of control variables (i.e. well locations and control settings) to maximize an objective function J. Net Present Value (NPV), considering only oil and water production/injection over the presumed life of the reservoir, is the selected objective function, defined as:

$$J(x,m) = \sum_{n=1}^{S} \left\{ \left[\sum_{j=1}^{N_P} \left(r_o q_{o,j}^n - r_{pw} q_{w,j}^n \right) - \sum_{k=1}^{N_I} \left(c_{wi} q_{wi,k}^n \right) \right] \times \frac{\delta t^n}{(1+b)^{t_n}} \right\} \qquad (1)$$

where x is the N_x dimensional vector of the control variables, m is the N_m dimensional vector of the uncertain reservoir description properties (e.g. porosity and permeability fields, fault transmissibility, oil-water contacts) quantified as the reservoir model realizations, n is the n^{th} time step of the reservoir simulation, S is the total number of simulation steps, δt^n is the length of n^{th} simulation step, t_n is the simulation time at the end of the n^{th} time step, b is the annual discount rate in decimal, and N_P and N_I are the number of producers and injectors, respectively. The cost coefficients r_o, r_{pw}, and c_{wi} denote the oil price, the water handling cost, and the water injection cost respectively; all in (USD/STB). $q_{o,j}^n$ and $q_{w,j}^n$ are the oil and water production rates of well j at time step n in STB/day. $q_{wi,k}^n$ is the water injection rate of well k at time step n in STB/day. Simulation runs are conducted using a commercial reservoir simulator (ECLIPSE-100) (Schlumberger 2017) to calculate the objective function for the specified set of control variables and model realizations. In this study, control variables x are scaled from the original domain $[x_{min}, x_{max}]$ to [0,1] (Eq. (2)) to eliminate the impact of different ranges of control variables at different optimization levels.

$$u_i = \frac{x_i - x_{min,i}}{x_{max,i} - x_{min,i}} \qquad (2)$$

Optimization methodology

SPSA is a stochastic optimization algorithm based on steepest ascent (or descent) while gradient is approximated using a randomly selected stencil (Spall 1992). Consider $J(x_k)$ to be the objective value, where x_k is the N_x dimensional vector of the control variables at iteration k. The gradient $g_k(x)$ is defined as the partial derivatives of the objective function $g_k(x) = \frac{\partial J}{\partial x} = \left[\frac{\partial J}{\partial x_1}, \frac{\partial J}{\partial x_2}, \dots, \frac{\partial J}{\partial x_{N_x}}\right]^T$, where $[.]^T$ represents a column vector. SPSA iteratively maximizes the objective function $J(x)$ using:

$$x_{k+1} = x_k + \alpha_k \hat{g}_k(x_k) \quad (3)$$

where $\hat{g}_k(x_k)$ is the stochastically estimated gradient of the objective function and $\alpha_k > 0$ is the step size at iteration k. To calculate $\hat{g}_k(x_k)$, Δ_k is defined as a vector of mutually independent, mean-zero random variables $\left\{\Delta_{k_1}, \Delta_{k_2}, \dots, \Delta_{k_{N_x}}\right\}$ using Bernoulli ± 1 symmetric distribution, satisfying the following conditions (Spall 1992):

$$\Delta_{k_i}^{-1} = \Delta_{k_i} \quad (4)$$

$$E\left|\Delta_{k_i}^{-1}\right| = E\left|\Delta_{k_i}\right| = 0 \quad (5)$$

where E represents the expected value. The stochastic gradient $\hat{g}_k(x_k)$ is then calculated using Δ_k and a positive scalar c_k:

$$\hat{g}_k(x_k) = \frac{J(x_k + c_k\Delta_k) - J(x_k - c_k\Delta_k)}{2c_k} \times \left[\frac{1}{\Delta_{k_1}}, \frac{1}{\Delta_{k_2}}, \dots, \frac{1}{\Delta_{k_{N_x}}}\right]^T \quad (6)$$

The convergence of the SPSA algorithm depends on the tuning parameters α_k and c_k. Spall (1998) suggested the following decaying sequences to calculate α_k and c_k to ensure a gradually refining search:

$$\alpha_k = \frac{a}{(\mathbb{A} + k + 1)^{\vartheta}} \quad (7)$$

$$c_k = \frac{c}{(k+1)^{\gamma}} \quad (8)$$

where a, c, $\mathbb{A}$, ϑ, and γ are positive, real numbers. The values of ϑ and γ are recommended to be 0.602 and 0.101 (Spall 1992). The stability constant $\mathbb{A}$ is recommended to be 5-10% of the expected, or allowed, number of iterations when optimizing continuous variables (Spall 2005). Jesmani et al. (2020) recommended using a larger $\mathbb{A}$ (e.g. $\mathbb{A}$ was set to 100 that is 33.3% of the 300 iterations) to achieve a more refined search in order to enhance the convergence of the algorithm in well placement optimization problems with discrete control variables. In this work, $\mathbb{A} = 100$ and $\mathbb{A} = 10$ is used for well placement and well control optimization levels, respectively. Sefat et al. (2016) recommended defining $0.1 \leq \alpha_0 \leq 0.5$ and c_{min} (i.e. when $k = k_{max}$) between 0.025 and 0.1 based on the complexity/noise of the search space. Initial sensitivity analysis in this work showed that faster convergence and more stable search process is achieved when $\alpha_0 = 0.5$ and $c_{min} = 0.08$ for both well location and control optimization.

The expectation of the stochastically estimated gradient ($\hat{g}_k(x_k)$) is the true gradient due to the random nature of Δ_k (Spall 1992). Wang et al. (2009), therefore, suggested using an averaged stochastic gradient calculated by use of an ensemble of perturbation vectors to improve the estimation of the search direction. Using the central difference formulation for gradient estimation, n_e independent samples of Δ_k are generated at each iteration, which results in $2 \times n_e$ objective function evaluations (Eq.(6)). The average stochastic gradient is then calculated by arithmetic averaging of the ensemble of n_e estimated gradients using the following equation:

$$\overline{\hat{g}_k(x_k)} = \frac{1}{n_e}\sum_{i=1}^{n_e} \hat{g}_i(x_k) \quad (9)$$

where $\overline{\hat{g}_k(x_k)}$ is the average stochastic gradient substituted for $\hat{g}_k(x_k)$ in Eq. (3). We observed that setting n_e between 3 to 5 provided a good quality of the estimated gradient for both well placement and control levels.

Uncertainty in reservoir description is generally captured by creating an ensemble (usually hundreds) of equally probable model realizations (Wang et al. 2012, Peters et al. 2010). Therefore, a fixed control vector (x) will produce different objective function values (J) when applied to different model realizations. Assuming n_c is a small subset of model realizations, selected as the representative of all

available realizations, $2 \times n_e \times n_c$ function evaluations are generally required at each iteration to estimate $\overline{\hat{g}_k(x_k)}$ using n_e estimated gradients (Eq. (9)) . Following Chen et al. (2009) and Fonseca et al. (2014) and considering mean of the selected realizations is the objective function, a 1:1 ratio can be used mapping one member of the ensemble of control variables perturbations to one member of the ensemble of selected model realizations. Assuming both ensembles have an equal number of members ($n_e = n_c$), a 1:1 ratio reduces the number of function evaluations to $2 \times n_e$ while preserving the accuracy of the estimated gradient. In this study, a 1:1 ratio is employed during both well placement and control optimization levels.

Realization selection and clustering

Selecting a small ensemble of model realizations as the representative of all available realizations can significantly reduce the computation time of robust optimization. A systematic approach is to tailor the realization selection process to the objective of the subsequent optimization stage. Wang et al. (2012) proposed projecting all model realizations to 2-D space while each dimension attributes to a temporal (e.g. cumulative oil production) or static (e.g. permeability, oil-water contact, original oil in place) property of the model, followed by clustering and selecting representative realizations from each cluster. They used normalized oil-water contact and cumulative oil production as model attributes when selecting representative realizations for well location optimization with the objective of maximizing NPV by enhancing reservoir sweep efficiency. Sefat et al. (2016) proposed using pairwise distance between water cut curves of all model realizations as similarity/dissimilarity measure when selecting realizations for well production optimization with the objective of increasing oil production by delaying water-breakthrough. Shirangi and Durlofsky (2016) also proposed to measure similarity/dissimilarity between model realizations using a low-dimensional feature vector containing a combination of static and dynamic (time-varying) model properties, tailored to the optimization objectives. They found that both static and dynamic model properties need to be considered when selecting realizations for well location optimization while dynamic properties become especially important in realization selection for well control optimization.

Optimal well locations are often functions of both static (geological) and dynamic (flow properties) features of the reservoir, hence at the well placement optimization level the realization selection is performed by creating a two-dimensional map where each model realization is characterized by its normalized permeability distance and the area under the field cumulative oil production curve. The permeability distance is defined as the Euclidean distance between the permeability field of a particular realization (m_i) and the average permeability field over all available realizations ($\bar{m}$) (i.e., $d_i = \|m_i - \bar{m}\|_2$ where $\|.\|$ represents the l_2-norm). K-means clustering (Seber 2009) is then performed to group all available realizations (n_r) into a small number of clusters (n_c) by iteratively finding the optimal cluster centers, i.e. $\tau_{opt} = \{\tau_1, \tau_2, \dots, \tau_{n_c}\}$, such that the summation of the distances of all n_r realizations from the nearest cluster center is minimized.

$$\tau_{opt} = \sum_{i=1}^{n_r} \min_{j=1,2,\dots,n_c} \|u_i - \tau_j\|^2 \qquad (10)$$

where τ_j is the center for cluster j, and u_i denotes the mapped realization. Each realization is then assigned to the nearest cluster center. Determining the optimum number of clusters is an ill-posed problem and mostly includes some form of intuition supported by a performance measure. The Silhouette value (Rousseeuw 1987) evaluates how well a data point is assigned to a particular cluster and is used as the clustering performance measure in this work. Assuming n_c clusters:

$$Sil_i = \frac{b_i - a_i}{\max(a_i, b_i)} \qquad (11)$$

$$a_i = d_{i,C(i)} \text{ and } b_i = \min_{C \neq C(i)} d_{i,C} \qquad (12)$$

$$d_{i,C} = \frac{1}{\#\ data\ points\ in\ cluster\ C} \sum_{l \epsilon C} D(u_i, u_l) \tag{13}$$

$$\overline{Sil}(n_c) = \frac{1}{n_r} \sum_{i=1,\dots,n_r} Sil_i \tag{14}$$

where Sil_i is the Silhouette value for data point i, $D(u_i, u_l)$ is the Euclidean distance between data point i and data point l, $d_{i,C}$ shows the average dissimilarity of data point i with all other data points in cluster C. Hence a_i indicates the average dissimilarity of data point i with all other data points within the same cluster while b_i shows the lowest average dissimilarity of point i with any point in any other cluster (i.e. the neighboring cluster which is the next best fit for point i). The optimum number of clusters ($n_{c_{opt}}$) is then determined by comparing the average silhouette value ($\overline{Sil}(n_c)$) for different number of clusters (n_c), where the maximum silhouette value indicates the best quality of clustering.

The objective of well control optimization level in this study is to improve oil recovery by delaying early water breakthrough in some wells. Hence, following Sefat et al. (2016), the realization selection at well control optimization level is started by calculating a pairwise distance between the well water cut curves of all model realizations, given by:

$$D(m_i, m_j) = \sum_{g=1}^{n_p} \int_{t=0}^{t_f} \left(f_{wc_g}(m_i, t) - f_{wc_g}(m_j, t) \right) dt \tag{15}$$

where $f_{wc_g}(m_i, t)$ is the water cut in the g^{th} production well as a response of model i (m_i) at time t, n_p is the total number of production wells, and t_f is the final production time. The $n_r \times n_r$ dissimilarity matrix is then projected into two-dimensional space using multidimensional scaling (MDS) (Borg and Groenen 2003), preserving the Euclidean distance between data points in 2D as close as possible to the distance measured in the original space (Eq. (15)). K-means clustering followed by average silhouette value analysis is performed to group model realizations into $n_{c_{opt}}$ clusters, similar to well placement optimization level. At both optimization levels, the realization closest to the center of each cluster is selected as the representative of that cluster (following Scheidt and Caers (2009) and Sefat et al. (2016)).

Multi-Solution Optimization Framework (MSOF) for well placement and control

Fonseca et al. (2014) and Haghighat Sefat (2016) showed that in optimization problems with a large number of control variables, the search space is characterized by several local optima with objective values close to each other. Therefore, the developed MSOF explores the search space to identify multiple sets of solutions with distinctly different control variables but close-to-optimum objective values. The multiple sets of solutions can be considered as realizations of the (uncertain) control variables. A similar realization selection approach, as the one explained in the previous section, can then be employed to select an ensemble of representative optimal solutions from each optimization level.

Solutions with low objective function values ($E(NPV)$) or with control variables values close to the optimal solution already selected are not good for the representative ensemble of optimal solutions from each optimization level. Hence, only the representative solutions with distinct differences in decision variables are selected from the top cases with objective values greater than a specified threshold, defined as p% of the maximum objective value (J_{max}) achieved. The optimal value of p (p_{opt}%) depends on two competing criteria: distinct dissimilarity of the selected solutions, and proximity of the objective value of the selected cases to the maximum objective value. Selecting a large percentage of cases at each level (e.g. the extreme case of all cases) captures the maximum diversity between optimization scenarios. However, the selected cases do not all have the potential to achieve a close-to-optimum objective value after the next level of optimization and therefore do not qualify as an acceptable final solution. In this study, a sensitivity analysis showed that selecting $p_{opt} = 0.8$ at each optimization level (i.e. all cases with objective values in the range of $[p_{opt} \times J_{max}, J_{max}]$ are selected, where J_{max} denotes

the maximum objective value achieved) provides the best performance in both sufficiently capturing the ensemble diversity and providing close-to-optimum objective values.
The similarity/dissimilarity of the selected solutions are measured as a pairwise distance between their corresponding control variable vectors, normalized into [0,1] using Eq. (2). At well placement optimization level, the employed approach calculates distances between reservoir grids with active wells irrespective of well names (Salehian et al. 2020) while conventional Euclidean distance is used at the well control optimization level. The selected solutions are then projected onto two-dimensional space using MDS followed by k-means clustering, accompanied by average Silhouette analysis to identify optimum number of clusters. One representative solution is then selected from each cluster, resulting in $n_{c_{opt}}$ representative solutions, to be transferred to the next optimization level.

Case study – Brugge model

Brugge (model) is a benchmark reservoir model based on a North Sea field (Peters et al. 2010). The model consists of 139 × 48 × 9 (total of 60,048) grid blocks of which approximately 45,000 are active. The reservoir permeability is moderately heterogeneous. In this example, the field is developed with five vertical producers and five vertical injectors all of which are fully perforated in all layers. The total production time is 30 years. Figure 1 shows the top structure of the model with the base case well locations. The uncertainty in the model description is quantified by 104 equiprobable realizations of the permeability, porosity, and net-to-gross (NTG) value distribution (Peters et al. 2013).

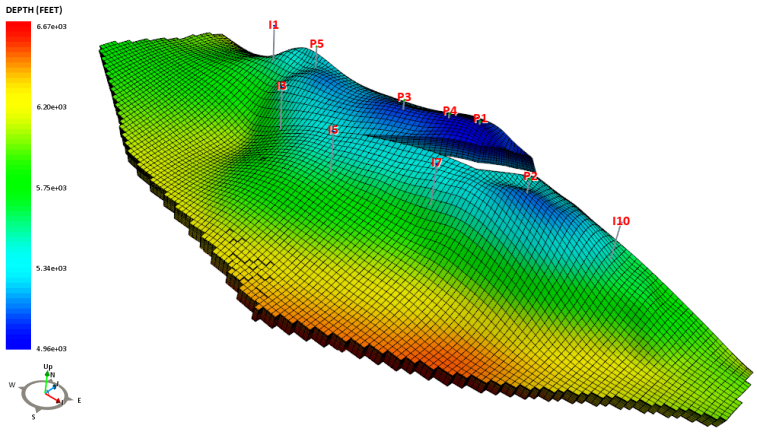

***Figure 1**-Top structure of the Brugge model.*

The objective function, NPV (Eq. (1)), is calculated using the economic parameters provided in Table 1. 150 and 300 iterations are performed at well placement and control optimization levels, respectively. Top (i, j) locations of the wells are optimized during well location optimization level, which results in $10 \times 2 = 20$ control variables. A minimum inter-well distance constraint of $200\ m$ (equivalent to 2 grid blocks) is imposed during well placement optimization level using a penalty method following Lu et al. (2017a). The producers are all controlled by Bottom Hole Pressure (BHP) varying between 725 and $1595\ psi$, while the injectors are each controlled by water injection rate varying between 0 and $6289\ STB/day$. The producers are shut when their water cut exceeds the economic value of 90% calculated using Table 1 economic parameters. 30 control steps (of 1 year each) is considered during well production/injection control resulting in total of $30 \times 10 = 300$ control variables.

***Table 1**-Economic parameters for calculating NPV*

Parameter	Value
Oil price	50 USD/STB
Water production cost	6 USD/STB
Water injection cost	3 USD/STB
Yearly discount rate	10%

Figure 2 shows the two-dimensional map of model realizations based on the normalized permeability distance and cumulative oil production. The optimum number of clusters is identified to be 4 ($n_{c_{opt}} = 4$) based on the average Silhouette analysis (Figure 3) as the max value is achieved with four clusters. The realization closest to the center of each cluster is selected as the cluster representative (Figure 4) and the selected realizations are employed during the robust, well location optimization level.

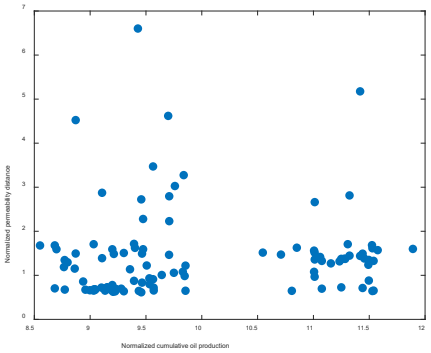

***Figure 2**-Two-dimensional map of all realizations based on permeability distance and cumulative oil production.*

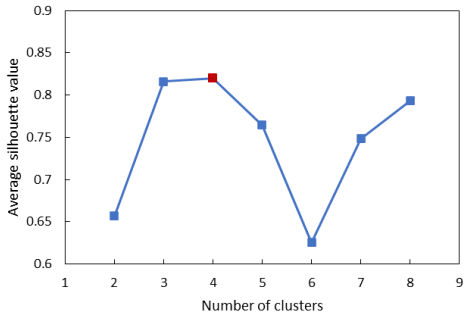

***Figure 3**-Average Silhouette value of all data points for different number of clusters in k-means.*

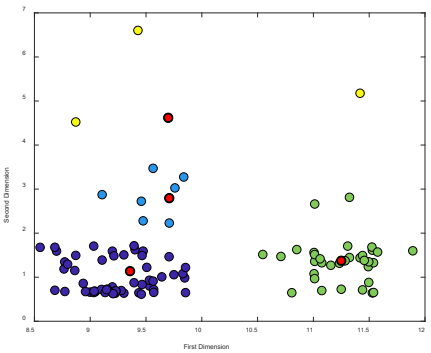

***Figure 4**-K-means clustering of reservoir model realizations considering four clusters, at well placement optimization level. Red points show the cluster representatives.*

Figure 5 shows the improvement in mean NPV of the selected realizations during well placement optimization iterations. The dissimilarities between the top selected well location solutions, within an E(NPV) shortfall of 20% as compared to the max case, are measured followed by projection on 2D using MDS (Figure 6). Each data point in Figure 6 represents a well location solution with the color showing E(NPV) over selected realizations confirming that a close to maximum objective value can be achieved by different well location solutions. The optimum number of clusters is identified to be 4 (Figure 7-left). The solution with the maximum NPV is selected as the representative of each cluster

(shown by red points in Figure 7-right), considering the objective of choosing solutions with high objective values.

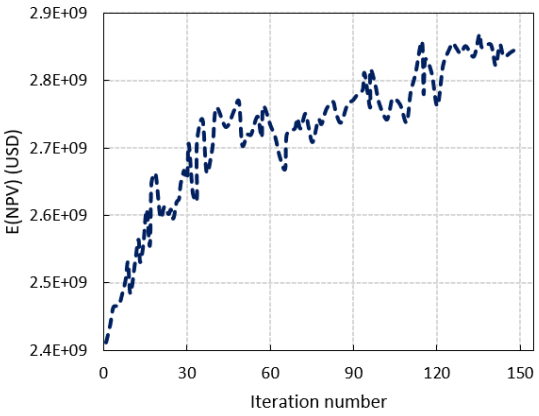

***Figure 5**-Expected objective value of the selected ensemble of realizations during well placement optimization.*

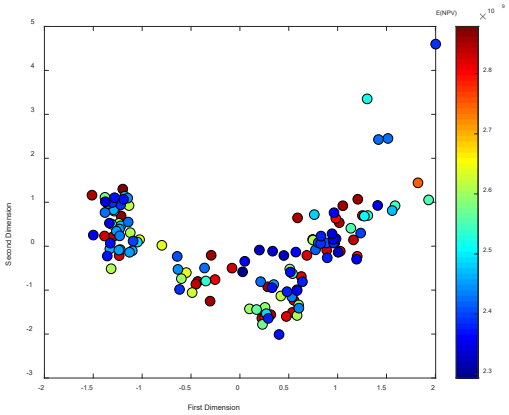

***Figure 6**-Projection of selected well placement solutions into a two-dimensional space using MDS (color shows objective value of each solution).*

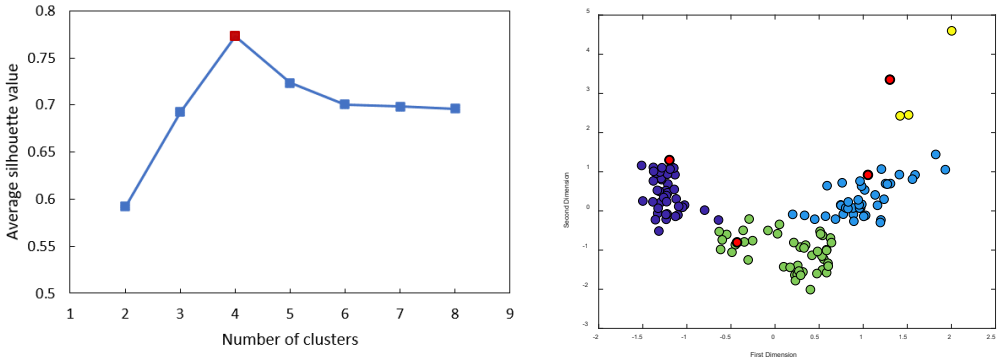

***Figure 7**- (Left)Mean Silhouette value analysis for the selected well placement solutions (Right) K-means clustering of the selected well placement solutions considering four clusters. Red points show the cluster representatives.*

Figure 8 shows the representative well placement solutions, named as L_1, L_3, L_4, and L_{64}, where subscripts denote the ranking of the solutions based on their $E(NPV)$ over the selected ensemble of realizations. Note that the case with the maximum objective value (L_1), i.e. the optimal solution of the classic single-solution approach, is automatically selected as a representative solution. Figure 9 shows the Probability Density Function (PDF) and Cumulative Density Function (CDF) when the selected

well placement solutions are applied to all model realizations as compared to the base case, while Table 2 shows the corresponding mean and standard deviations. The bi-modal shape of PDF in Figure 9 stems from the relationship between the porosity and permeability of realizations derived from the well logs from the truth models (Peters et al. 2013). A very similar global performance is observed by the selected ensemble of solutions (Table 2) while they provide a reasonable degree of flexibility in the well locations (Figure 8). It should be noted that a suboptimal member of the selected ensemble of solutions (e.g. L_4 here) can potentially provide a better global performance over all realizations, showing the robustness of the developed multi-solution framework.

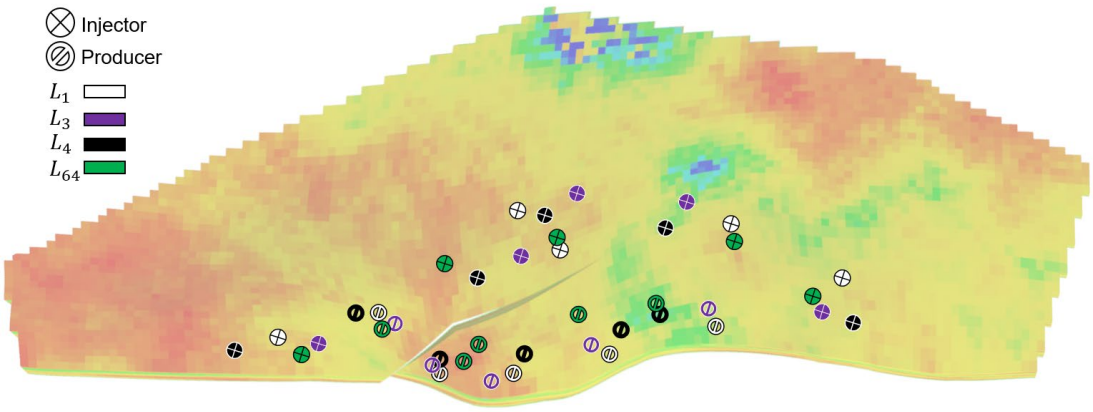

***Figure 8**-Four optimal well locations obtained by MSOF*

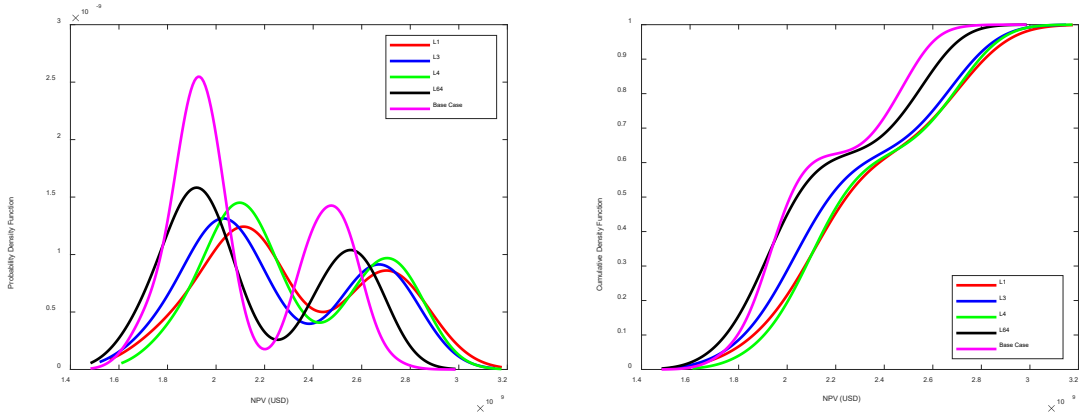

***Figure 9**-(left) PDF (right) CDF for the optimal well placement solutions obtained by MSOF as compared to the base case*

***Table 2**-Mean and standard deviation of the optimal well placement solutions over all realizations*

Solution	$E(NPV) \times 10^9$	$\sigma(NPV) \times 10^8$
Base Case	1.93	2.55
L1	2.30	3.64
L3	2.26	3.66
L4	2.31	3.42
L64	2.15	3.45

A new set of reservoir model realizations are selected, based on the distance measure described before (Eq. (15)), for each member of the ensemble of optimal well location solutions prior to well control optimization. Figure 10 shows the clustering performance, where the optimal number of clusters are determined using average Silhouette value analysis for each case. The control settings for each optimal well location solutions are then individually optimized at the next optimization level. Figure 11 shows improvement in the *E(NPV)* of the corresponding ensemble of reservoir model realizations during 300 iterations of well control optimization for each optimal well location solutions.

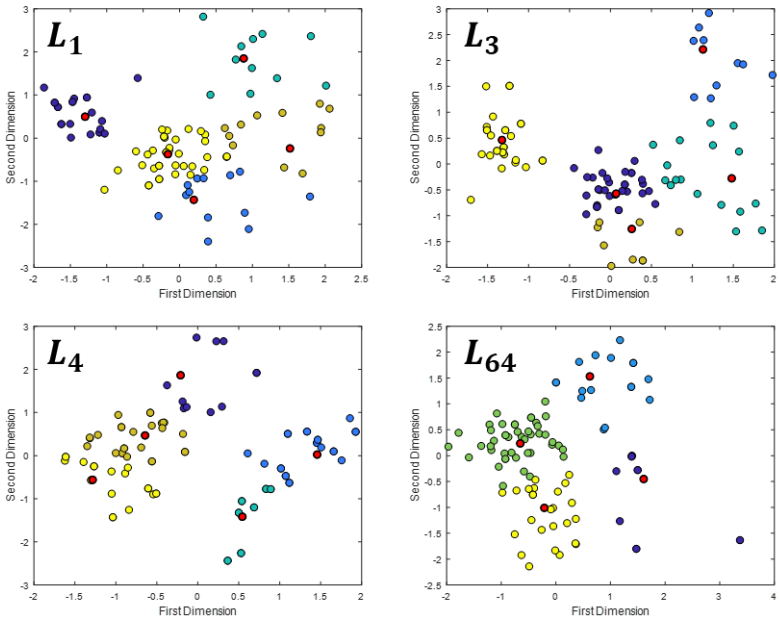

Figure 10- *K-means clustering for reservoir model realization selection for each member of the ensemble of optimal well location solutions prior to well control optimization. Red points show the cluster representatives.*

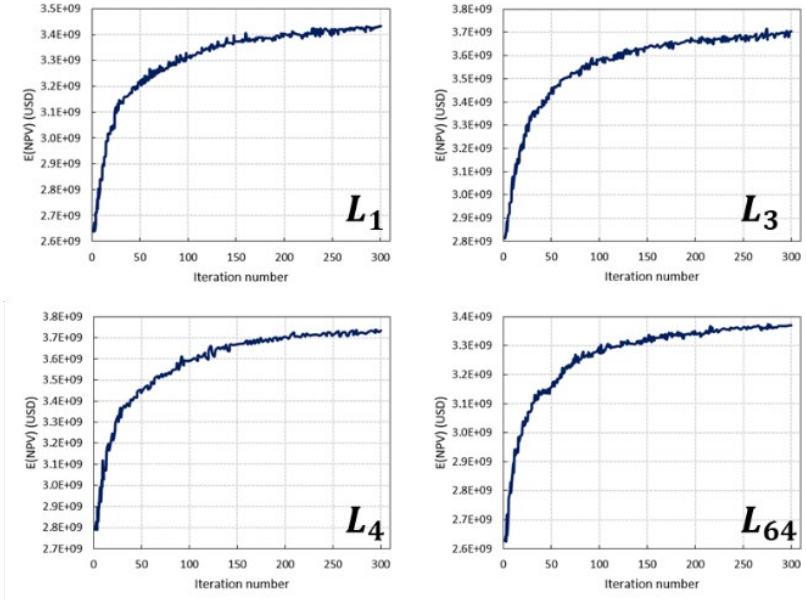

Figure 11- *E(NPV) of the corresponding ensemble of reservoir model realizations during well control optimization for each optimal well placement scenario.*

A similar clustering approach is applied to the control solutions where an ensemble of representative solutions is selected from the top cases within an *E(NPV)* shortfall of less than 20% w.r.t. the max case. Conventional Euclidean distance is used to measure the dissimilarity between control scenarios followed by MDS to map them into two-dimensional space (Figure 12). Figure 13 shows the k-means clustering where the optimum number of clusters is determined by average Silhouette value analysis. The control scenario with the maximum NPV is then selected from each cluster as the representative of that cluster, resulting in a total of twelve optimal well control scenarios for all four well placement strategies.

The optimization trajectory as a result of using a gradient-based algorithm for optimizing well control (i.e. a continuous variable) is clearly shown in Figure 12 while a more scattered search is performed during well location optimization level with discrete variables (Figure 6). This characteristic of the

optimization algorithm limits the exploration of the search space. Further research is currently ongoing to achieve the maximum level of diversity in close-to-optimum solutions by enhancing the exploration of the search space, especially at the well location optimization level unlike at the well control one where lower diversity of selectable solutions is generally accepted due to the flexible nature of the well control operations.

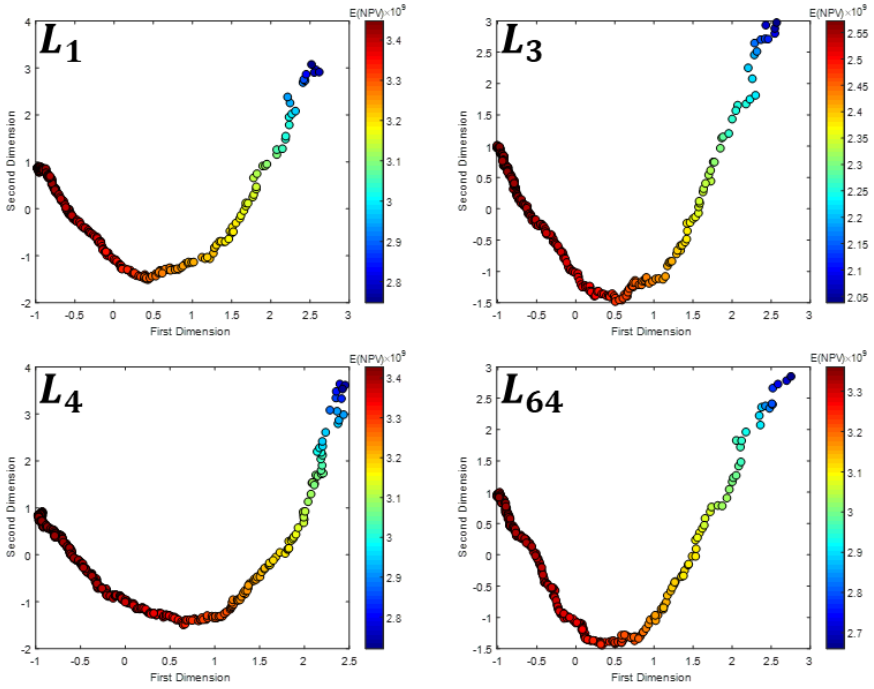

Figure 12- *Projection of selected well control solutions corresponding to four optimal well locations into a two-dimensional space using MDS.*

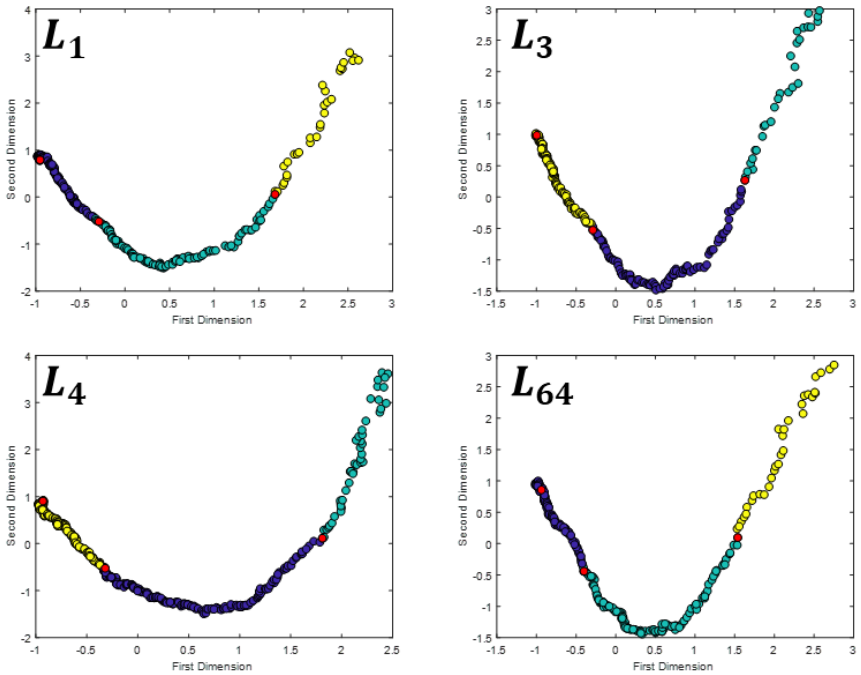

Figure 13 *- K-means clustering followed by selection of the representative well control solutions, for each optimal well location. The optimal number of clusters for each ensemble is identified by average Silhouette value analysis.*

Table 3 shows the mean and standard deviation of the final ensemble of close-to-optimum scenarios over all realizations, where e.g. $L3.C268$ denotes the 268th control scenario, ranked based on $E(NPV)$ during the well control optimization, using well location solution L_3. It can be seen that $L4.C231$

delivers the greatest global performance (over all reservoir model realizations) while only $L1.C1$ would be obtained as the single optimal solution using traditional, single-solution-transfer optimization frameworks. Moreover, a sub-optimal control scenario (i.e. with lower expected objective function value over the selected ensemble of realizations) could deliver higher global performance (over the full ensemble of realizations)(e.g. $E(NPV)_{L1.C154} > E(NPV)_{L1.C1}$ and $E(NPV)_{L4.C231} > E(NPV)_{L4.C1}$), demonstrating the robustness of the developed MSOF and it efficiency in exploration of the search space .

The sequential optimization loop was terminated since no further improvements in the expected objective value was achieved at the second loop. $L1.C154$, $L3.C150$, $L4.C231$, and $L64.C1$ are selected as the optimal control scenarios with the highest $E(NPV)$ for each well location solution. Figure 14 shows the CDF of selected solutions compared to the base case while Figure 15 and Figure 16 show the injection rate and BHP for these scenarios, respectively. A realistic level of variability in the optimal location and control is observed while the objective value varies in a relatively small range [2.80×10^9 - 3.08×10^9 USD], indicating the possibility of achieving a close-to-optimum objective value via different field development/control scenarios.

Table 3- *Mean and standard deviation of the optimal solutions over 104 realizations.*

Solution	$E(NPV)\times10^9$	$\sigma(E(NPV)\times10^8)$	Solution	$E(NPV)\times10^9$	$\sigma(E(NPV)\times10^8)$
$L1.C1$	2.85	4.60	$L4.C1$	2.88	4.71
$L1.C154$	3.00	4.59	$L4.C231$	3.08	4.76
$L1.C265$	2.78	4.42	$L4.C246$	2.85	4.45
$L3.C1$	2.84	4.56	$L64.C1$	2.80	4.61
$L3.C150$	2.93	4.71	$L64.C126$	2.76	4.57
$L3.C268$	2.70	4.39	$L64.C263$	2.58	4.32

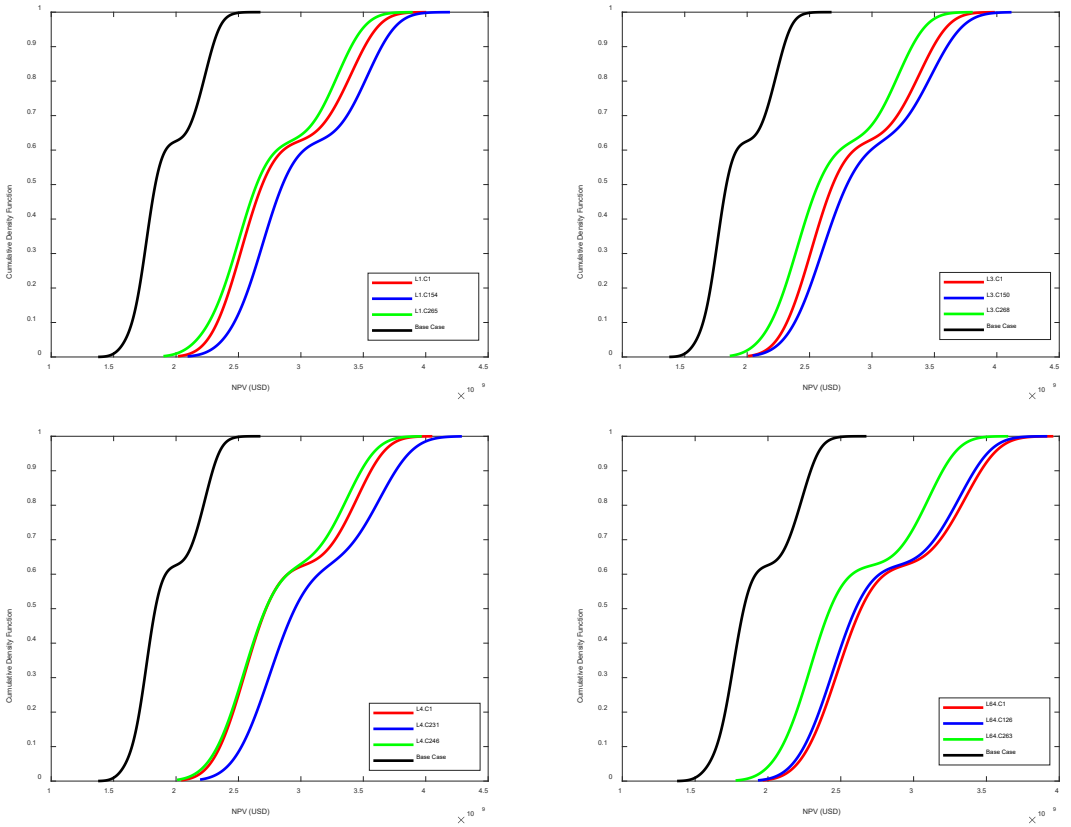

Figure 14 *– CDF of the representative control solutions based on four optimal well locations.*

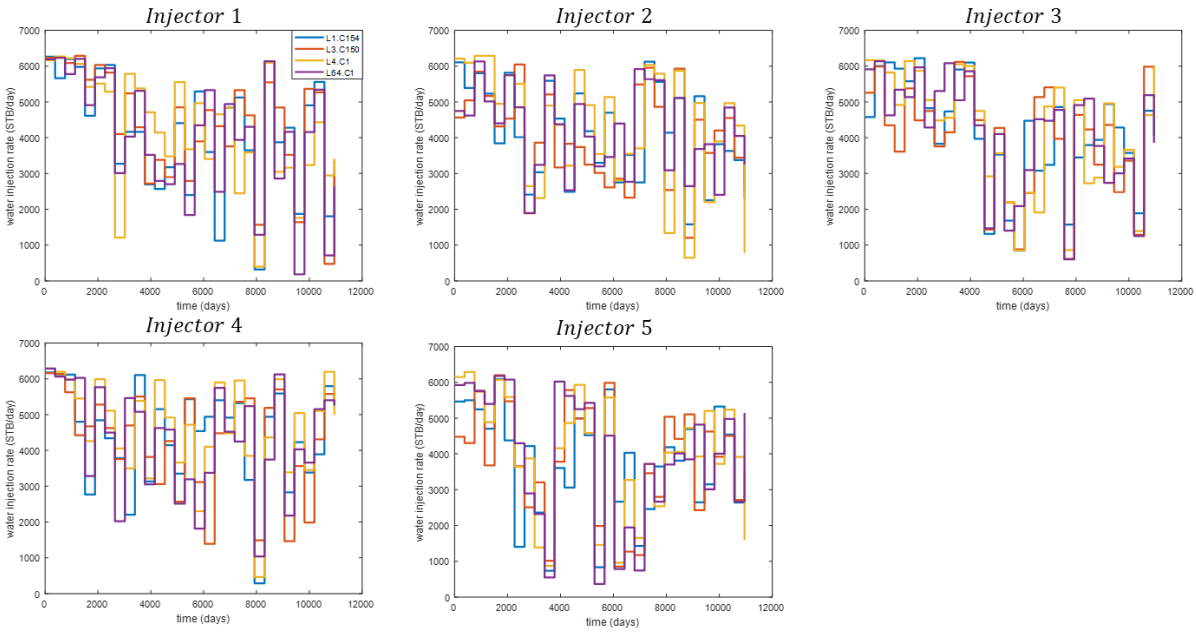

***Figure 15**-Optimal water injection rates based on four optimal well locations, obtained by MSOF.*

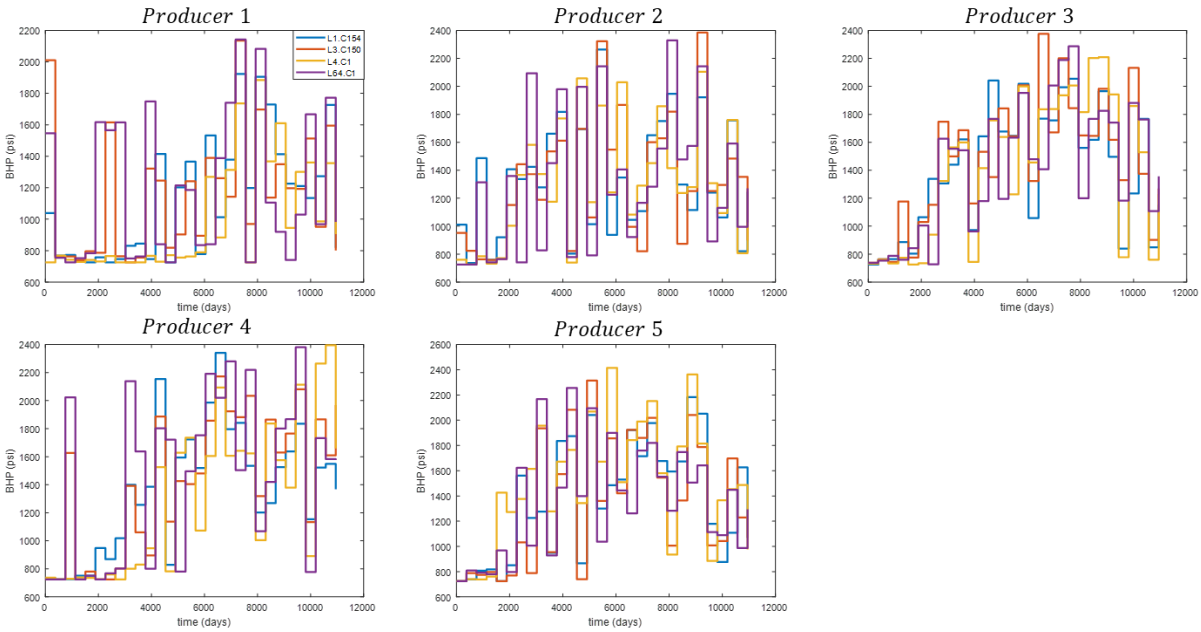

***Figure 16**-Optimal BHP values based on four optimal well locations, obtained by MSOF.*

Conclusions

A robust multi-solution optimization framework is developed to provide the operational flexibility by offering multiple robust field development and control scenarios by efficient exploration of the search space. Systematic clustering techniques were developed to select an ensemble of realizations to capture the underlying model uncertainties, as well as an ensemble of solutions with enough differences in control variables but close-to-optimum objective values, at each optimization level. SPSA was employed in a multi-level, sequential, iterative approach to find optimal well placement and control scenarios. The proposed framework was applied to a benchmark case study.

- The systematic realization selection process, tailored to the objective of the subsequent optimization stage, efficiently represented the characteristics of full ensemble of realizations while significantly reducing the computation time of robust optimization.

- Estimation of the stochastic gradients at each iteration using a 1:1 ratio between the ensemble of control variables perturbations and the ensemble of selected model realizations substantially reduced the computation time while preserving the accuracy of approximated gradient.
- Using a gradient-based algorithm for optimizing well control with continuous variables resulted in a specific optimization trajectory, while a more scattered search was performed during well location optimization level with discrete variables.
- Multiple optimal well placement and control solutions with close-to-optimum objective values but different decision variables were obtained.
- Selected suboptimal location/control solutions over the small subset of realizations can outdo the optimal one when applied to all realizations, highlighting the advantage of here-developed MSOF in order to provide a more robust solution and the much-needed operational flexibility in field optimization problems.

Acknowledgements
Authors appreciate the sponsors of the "Value from Advanced Wells II" Joint Industry Project at Heriot-Watt University for providing financial support and Schlumberger Information Solutions for allowing academic access to their software.

References
Al-Ismael, Menhal, Awotunde, Abeeb, Al-Yousef, Hasan et al. 2018. A Well Placement Optimization Constrained to Regional Pressure Balance. *Proc.,* SPE Europec featured at 80th EAGE Conference and Exhibition.
Almeida, Luciana Faletti, Vellasco, Marley MBR, and Pacheco, Marco AC. 2010. Optimization system for valve control in intelligent wells under uncertainties. *Journal of Petroleum Science and Engineering* **73** (1-2): 129-140.
Borg, Ingwer and Groenen, Patrick. 2003. Modern multidimensional scaling: Theory and applications. *Journal of Educational Measurement* **40** (3): 277-280.
Chen, Chaohui, Li, Gaoming, and Reynolds, Albert. 2012. Robust constrained optimization of short- and long-term net present value for closed-loop reservoir management. *SPE Journal* **17** (03): 849-864.
Chen, Yan, Oliver, Dean S, and Zhang, Dongxiao. 2009. Efficient ensemble-based closed-loop production optimization. *SPE Journal* **14** (04): 634-645.
Fonseca, Rahul Rahul-Mark, Chen, Bailian, Jansen, Jan Dirk et al. 2017. A stochastic simplex approximate gradient (StoSAG) for optimization under uncertainty. *International Journal for Numerical Methods in Engineering* **109** (13): 1756-1776.
Fonseca, RM, Leeuwenburgh, O, Van den Hof, PMJ et al. 2014. Ensemble-based hierarchical multi-objective production optimization of smart wells. *Computational Geosciences* **18** (3-4): 449-461.
Forouzanfar, Fahim, Poquioma, Walter E, and Reynolds, Albert C. 2016. Simultaneous and sequential estimation of optimal placement and controls of wells with a covariance matrix adaptation algorithm. *SPE Journal* **21** (02): 501-521.
Güyagüler, Baris, Horne, Roland N, Rogers, Leah et al. 2002. Optimization of well placement in a Gulf of Mexico waterflooding project. *SPE Reservoir Evaluation & Engineering* **5** (03): 229-236.
Haghighat Sefat, Morteza. 2016. *Proactive optimisation of intelligent wells under uncertainty*, Heriot-Watt University.
Harb, Ahmad, Kassem, Hussein, and Ghorayeb, Kassem. 2019. Black hole particle swarm optimization for well placement optimization. *Computational Geosciences*: 1-22.
Isebor, Obiajulu J, Durlofsky, Louis J, and Ciaurri, David Echeverría. 2014. A derivative-free methodology with local and global search for the constrained joint optimization of well locations and controls. *Computational Geosciences* **18** (3-4): 463-482.
Jesmani, M, Jafarpour, B, Bellout, MC et al. 2016. Application of simultaneous perturbation stochastic approximation to well placement optimization under uncertainty. *Proc.,* ECMOR XV-15th European Conference on the Mathematics of Oil Recoverycp-494-00133.
Jesmani, Mansoureh, Jafarpour, Behnam, Bellout, Mathias C et al. 2020. A reduced random sampling strategy for fast robust well placement optimization. *Journal of Petroleum Science and Engineering* **184**: 106414.

Jiang, Su, Sun, Wenyue, and Durlofsky, Louis J. 2019. A data-space inversion procedure for well control optimization and closed-loop reservoir management. *Computational Geosciences*: 1-19.
Li, Lianlin and Jafarpour, Behnam. 2012. A variable-control well placement optimization for improved reservoir development. *Computational Geosciences* **16** (4): 871-889.
Li, Lianlin, Jafarpour, Behnam, and Mohammad-Khaninezhad, M Reza. 2013. A simultaneous perturbation stochastic approximation algorithm for coupled well placement and control optimization under geologic uncertainty. *Computational Geosciences* **17** (1): 167-188.
Lu, Ranran, Forouzanfar, Fahim, and Reynolds, Albert C. 2017a. Bi-objective optimization of well placement and controls using stosag. *Proc.,* SPE Reservoir Simulation Conference.
Lu, Ranran, Forouzanfar, Fahim, and Reynolds, Albert C. 2017b. An efficient adaptive algorithm for robust control optimization using StoSAG. *Journal of Petroleum Science and Engineering* **159**: 314-330.
Lu, Ranran and Reynolds, AC. 2019. Joint Optimization of Well Locations, Types, Drilling Order and Controls Given a Set of Potential Drilling Paths. *Proc.,* SPE Reservoir Simulation Conference.
Peters, E, Chen, Y, Leeuwenburgh, O et al. 2013. Extended Brugge benchmark case for history matching and water flooding optimization. *Computers & Geosciences* **50**: 16-24.
Peters, Lies, Arts, Rob, Brouwer, Geert et al. 2010. Results of the Brugge benchmark study for flooding optimization and history matching. *SPE Reservoir Evaluation & Engineering* **13** (03): 391-405.
Rousseeuw, Peter J. 1987. Silhouettes: a graphical aid to the interpretation and validation of cluster analysis. *Journal of computational and applied mathematics* **20**: 53-65.
Salehian, Mohammad, Haghighat Sefat, Morteza, and Muradov, Khafiz. 2020. Development of a Multi-Solution Framework for Simultaneous Well Placement, Completion and Control Optimization. *SPE Europec featured at 82nd EAGE Conference and Exhibition*.
Sarma, Pallav, Aziz, Khalid, and Durlofsky, Louis J. 2005. Implementation of adjoint solution for optimal control of smart wells. *Proc.,* SPE reservoir simulation symposium.
Scheidt, Céline and Caers, Jef. 2009. Uncertainty quantification in reservoir performance using distances and kernel methods--application to a west africa deepwater turbidite reservoir. *SPE Journal* **14** (04): 680-692.
Schlumberger. 2017. ECLIPSE® User Manual.
Seber, George AF. 2009. *Multivariate observations*, Vol. 252: John Wiley & Sons.
Sefat, Morteza Haghighat, Elsheikh, Ahmed H, Muradov, Khafiz M et al. 2016. Reservoir uncertainty tolerant, proactive control of intelligent wells. *Computational Geosciences* **20** (3): 655-676.
Shirangi, Mehrdad G and Durlofsky, Louis J. 2016. A general method to select representative models for decision making and optimization under uncertainty. *Computers & geosciences* **96**: 109-123.
Shirangi, Mehrdad G, Volkov, Oleg, and Durlofsky, Louis J. 2018. Joint optimization of economic project life and well controls. *SPE Journal* **23** (02): 482-497.
Spall, James C. 1992. Multivariate stochastic approximation using a simultaneous perturbation gradient approximation. *IEEE transactions on automatic control* **37** (3): 332-341.
Spall, James C. 1998. Implementation of the simultaneous perturbation algorithm for stochastic optimization. *IEEE Transactions on aerospace and electronic systems* **34** (3): 817-823.
Spall, James C. 2005. *Introduction to stochastic search and optimization: estimation, simulation, and control*, Vol. 65: John Wiley & Sons.
Tavallali, Mohammad Sadegh, Bakhtazma, Farnoosh, Meymandpour, Ali et al. 2018. Optimal Drilling Planning by Considering the Subsurface Dynamics–Combing the Flexibilities of Modeling and a Reservoir Simulator. *Industrial & Engineering Chemistry Research*.
Van Essen, Gijs, Van den Hof, Paul, and Jansen, Jan-Dirk. 2011. Hierarchical long-term and short-term production optimization. *SPE Journal* **16** (01): 191-199.
Wang, Chunhong, Li, Gaoming, and Reynolds, Albert C. 2009. Production optimization in closed-loop reservoir management. *SPE journal* **14** (03): 506-523.
Wang, Honggang, Echeverría-Ciaurri, David, Durlofsky, Louis et al. 2012. Optimal well placement under uncertainty using a retrospective optimization framework. *Spe Journal* **17** (01): 112-121.
Zingg, David W, Nemec, Marian, and Pulliam, Thomas H. 2008. A comparative evaluation of genetic and gradient-based algorithms applied to aerodynamic optimization. *European Journal of Computational Mechanics/Revue Européenne de Mécanique Numérique* **17** (1-2): 103-126.